

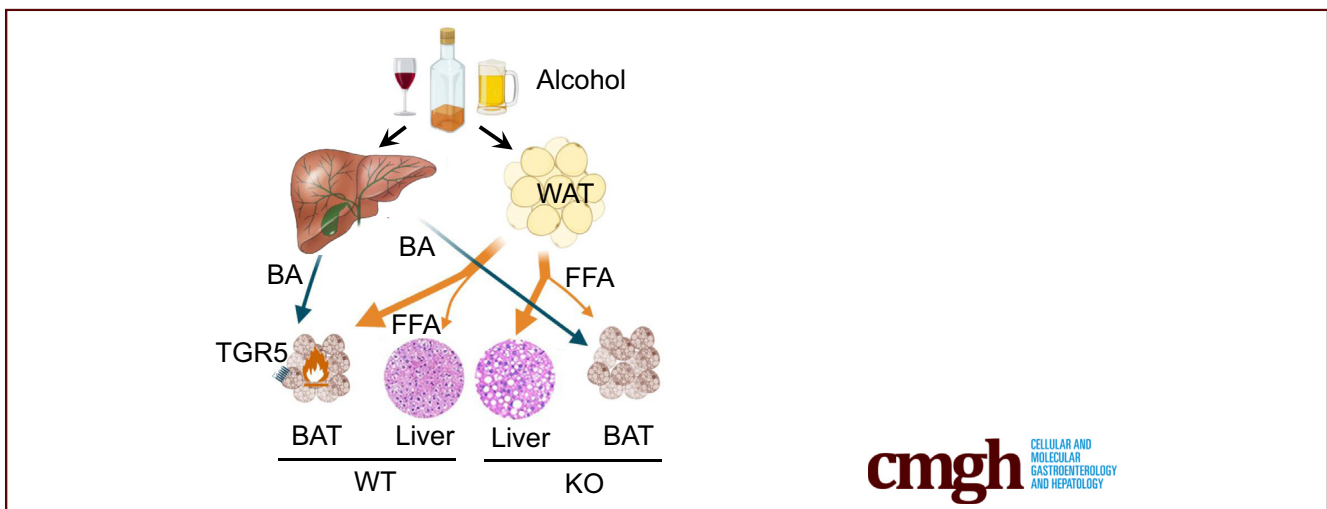
ORIGINAL RESEARCH

Bile Acid–Mediated Activation of Brown Fat Protects From Alcohol-Induced Steatosis and Liver Injury in Mice



Mingjie Fan,^{1,2} Yangmeng Wang,² Lihua Jin,² Zhipeng Fang,² Jiangling Peng,² Jui Tu,² Yanjun Liu,² Eryun Zhang,² Senlin Xu,^{2,3} Xiaoqian Liu,² Yuqing Huo,⁴ Zhaoli Sun,⁴ Xiaojuan Chao,⁵ Wen-Xing Ding,⁵ Qingfeng Yan,¹ and Wendong Huang^{2,3}

¹College of Life Science, Zhejiang University, Hangzhou, Zhejiang, China; ²Department of Diabetes Complications and Metabolism, ³Graduate School of Biological Science, Beckman Research Institute, City of Hope National Medical Center, Duarte, California; ⁴Department of Surgery, The Johns Hopkins University School of Medicine, Baltimore, Maryland; ⁵Department of Pharmacology, Toxicology and Therapeutics, University of Kansas Medical Center, Kansas City, Kansas



SUMMARY

Bile acid signaling ameliorates alcohol-associated liver disease by enhancing Takeda G-protein–coupled bile acid receptor 5–mediated brown adipose tissue thermogenesis, thereby reducing the absorption of free fatty acids into liver, which were released from white adipose tissue after alcohol consumption. A Takeda G-protein–coupled bile acid receptor 5–specific agonist may provide a therapy for alcohol-associated liver disease by enhancing brown adipose tissue thermogenesis.

BACKGROUND & AIMS: Alcohol-associated liver disease (AALD) is one of the most common causes of liver injury and failure. Limited knowledge of the mechanisms underlying AALD impedes the development of efficacious therapies. Bile acid (BA) signaling was shown to participate in the progression of AALD. However, the mechanisms remain poorly understood.

METHODS: C57BL/6J wild-type (WT), Takeda G-protein–coupled bile acid receptor 5 (TGR5) knockout (KO) and brown adipose tissue (BAT)-specific TGR5 knockdown mice were subjected to ethanol feeding–induced AALD. Liver samples

from alcoholic hepatitis patients were used to examine the BA circulation signaling. Human Embryonic Kidney Cells 293 were used for the TGR5 reporter assay. 23(S)-methyl-lithocholic acid was used as a molecular tool to confirm the regulatory functions of BAT in the AALD mouse model.

RESULTS: Ethanol feeding increased the expression of the thermogenesis genes downstream of TGR5 in BAT of WT, but not TGR5 KO, mice. TGR5 deficiency significantly blocked BAT activity and energy expenditure in mice after ethanol feeding. Alcohol increased serum BA levels in mice and human beings through altering BA transportation, and the altered BAs activated TGR5 signaling to regulate metabolism. Compared with ethanol-fed WT mice, ethanol-fed TGR5 KO mice showed less free fatty acid (FFA) β -oxidation in BAT, leading to higher levels of FFA in the circulation, increased liver uptake of FFAs, and exacerbated AALD. BAT-specific TGR5 knockdown mice showed similar results with TGR5 KO mice in AALD. Agonist treatment significantly activated TGR5 signaling in BAT, increased thermogenesis, reduced serum FFA level, and ameliorated hepatic steatosis and injury in AALD mice, while these effects were lost in TGR5 KO mice.

CONCLUSIONS: BA signaling plays a protective role in AALD by enhancing BAT thermogenesis. Targeting TGR5 in BAT may be a promising approach for the treatment of AALD. (*Cell Mol*

Gastroenterol Hepatol 2022;13:809–826; <https://doi.org/10.1016/j.jcmgh.2021.12.001>

Keywords: Alcohol-Associated Liver Disease (AALD); TGR5 (GPBAR1); BAT-Liver Crosstalk; Thermogenesis.

Alcohol-associated liver disease (AALD) is a leading cause of liver failure worldwide.¹ Ethanol perturbs almost all aspects of hepatic lipid metabolism.² AALD progresses from alcoholic steatosis to alcoholic steatohepatitis, characterized by chronic hepatic inflammation, and leads to fibrosis, cirrhosis, and, in certain cases, hepatocellular carcinoma.³ Alcoholic steatosis is the earliest and most common response of the liver to moderate or large doses (ie, binge drinking) of alcohol, as well as to chronic ethanol consumption.⁴ Although therapies are being developed for AALD, they have limited efficacy and safety issues.⁵ In light of this, there is an urgent need to understand the molecular mechanisms driving AALD to develop effective preventive and therapeutic approaches for AALD.

In addition to facilitating the absorption of lipids and other nutrients, bile acids (BAs) play a critical role as signaling molecules in metabolic regulation.⁶ Recently, serum BAs were reported to be increased significantly in individuals with alcoholic hepatitis (AH).⁷ In rodents, ethanol consumption altered BA biosynthesis and transporters.^{8–10} Emerging evidence has shown that BA signaling contributes to the development of AALD. For example, alcohol feeding aggravated liver inflammation and injury in mice deficient for cholesterol 7 α -hydroxylase (Cyp7a1), a rate-limiting enzyme in BA synthesis.¹¹ In addition, deficiency in the nuclear BA receptor Farnesoid X receptor (FXR) exacerbated chronic alcoholic liver injury.¹² BAs also activate signaling downstream of cell membrane-associated G-protein-coupled BA receptor 1 (GPBAR1 or TGR5). TGR5 is highly expressed in the gallbladder, liver, and intestine. In the liver, TGR5 exerts anti-inflammatory effects, protects cholangiocytes from BA-induced toxicity, promotes cholangiocyte secretion and proliferation, and reduces portal perfusion pressure.^{13,14} TGR5 also protects the liver from BA overload during liver regeneration and markedly reduces lipopolysaccharide-induced cytokine production in primary macrophages.¹⁵ In the intestine, TGR5 activates cyclic adenosine monophosphate (cAMP) signaling to stimulate glucagon-like peptide-1 secretion, leading to reduced hepatic glucose production.¹⁶ Evidence in vitro has shown that TGR5 activation suppresses the expression of interleukin (IL)1 β and tumor necrosis factor- α (TNF- α) in the murine macrophage cell line RAW264.7 and murine Kupffer cells.¹⁷ Although these important physiological regulations of TGR5 in liver have been well investigated, the mechanisms by which TGR5 activation significantly protects against AALD remain poorly understood.

Alcohol administration increased the expression of uncoupling protein 1 (UCP1) in brown adipose tissue (BAT) and activated UCP1-mediated thermogenesis, while UCP1 deficiency profoundly increased the severity of alcoholic liver steatosis, injury, and fibrosis in mice.¹⁸ These data hint

at an unrecognized role of BAT in AALD development. TGR5 also is highly expressed in BAT, and BA-activated TGR5 signaling increases cAMP, which itself activates type 2 iodothyronine deiodinase (Dio2) in BAT, leading to mitochondrial uncoupling and enhanced thermogenesis.¹⁹ These findings support the hypothesis that BAT TGR5 protects against AALD through crosstalk with the liver. Herein, we tested this hypothesis in ethanol-fed TGR5 knockout (KO) mice, BAT-specific TGR5 knockdown (KD) mice, and wild-type (WT) mice.

Results


TGR5 Deficiency Blocks Ethanol-Stimulated BAT Thermogenesis

TGR5 plays a critical role in BAT thermogenesis through TGR5–cAMP–Dio2 signaling.²⁰ To test if TGR5 contributes to alcohol-induced BAT thermogenesis, we compared a chronic-plus-one-binge ethanol feeding-induced AALD model in WT and TGR5 KO mice. First, we measured the messenger RNA (mRNA) levels of key downstream genes. Expression of Dio2, peroxisome proliferator-activated receptor γ coactivator 1 α , and PR domain containing 16 were increased significantly after ethanol feeding in WT mice (EtOH-WT), but not in ethanol-fed TGR5 KO mice (EtOH-KO) (Figure 1A). Although the mRNA and protein levels of UCP1 were increased after ethanol feeding in both WT and TGR5 KO mice, their levels were overall less in EtOH-KO animals (Figure 1A and B). H&E staining and UCP1 immunostaining confirmed more lipid accumulation and weaker UCP1 signal in the BAT of EtOH-KO mice than EtOH-WT mice (Figure 1C). Predictably, ethanol feeding significantly increased energy expenditure in WT mice. However, absence of TGR5 dramatically blocked ethanol-stimulated energy expenditure (Figure 1D). An AALD model of male mice showed similar results in the expression of genes involved in thermogenesis and β -oxidation in BAT (Figure 1E and 1F). These results show that TGR5 is required in alcohol-induced energy expenditure.

Altered BA Profile After Alcohol Intake Activates TGR5 in BAT

Serum BA levels are increased significantly in individuals and rodents after alcohol consumption,^{7–10} and BA-

Abbreviations used in this paper: AALD, alcohol-associated liver disease; AH, alcoholic hepatitis; ALT, alanine aminotransferase; BA, bile acid; BAT, brown adipose tissue; cAMP, cyclic adenosine monophosphate; CD, cluster of differentiation; CYP7A1, cholesterol 7 α -hydroxylase; Dio2, type 2 iodothyronine deiodinase; DY284, 23(S)-methyl-lithocholic acid; FFA, free fatty acid; FXR, Farnesoid X receptor; IL, interleukin; KD, knockdown; KO, knockout; mRNA, messenger RNA; NEFA, nonesterified free fatty acid; PCR, polymerase chain reaction; TGR5, Takeda G-protein-coupled bile acid receptor 5; TNF- α , tumor necrosis factor- α ; UCP1, uncoupling protein 1; WAT, white adipose tissue; WT, wild-type.

 Most current article

© 2021 The Authors. Published by Elsevier Inc. on behalf of the AGA Institute. This is an open access article under the CC BY-NC-ND license (<http://creativecommons.org/licenses/by-nc-nd/4.0/>).

2352-345X

<https://doi.org/10.1016/j.jcmgh.2021.12.001>

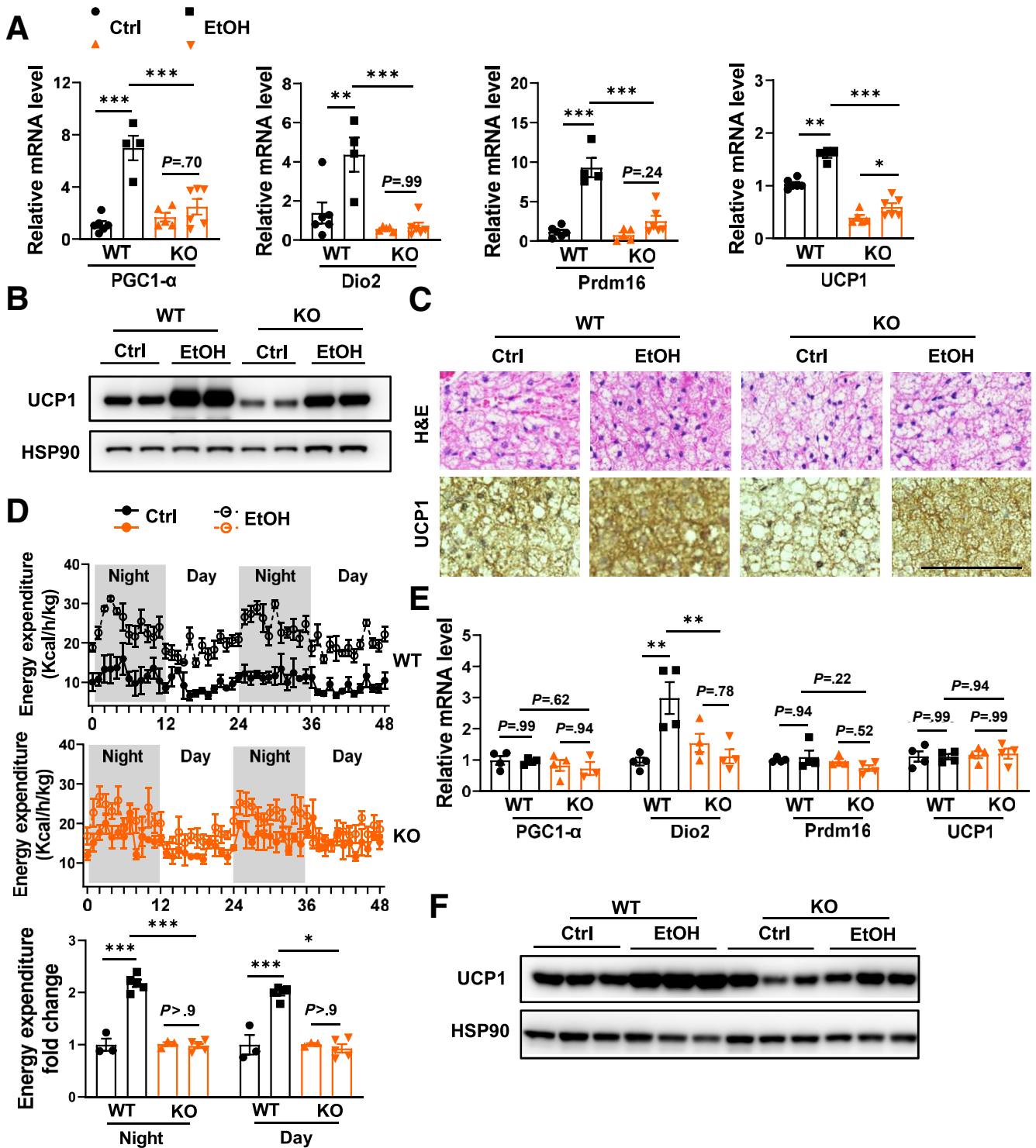


Figure 1. TGR5 deficiency blocks ethanol-stimulated BAT thermogenesis. Eight- to 10-week-old (A–D) female or (E and F) male WT and TGR5 KO mice were subjected to chronic-plus-one-binge ethanol feeding to induce AALD. (A) Relative mRNA levels of thermogenesis genes in BAT. n = 5–6. (B) Representative images of Western blot analysis of UCP1 protein in BAT. (C) Representative images of BAT sections by H&E staining and UCP1 immunostaining, respectively. (D) Energy expenditure of mice over a 48-hour period on the 11th and 12th days of the experiment. n = 3 for control groups (Ctrl) and n = 5 for ethanol-fed groups (EtOH). (E) Relative mRNA levels of thermogenesis genes in BAT in male mice. n = 4. (F) Western blot analysis of protein levels of UCP1 in BAT in male mice. Values are means ± SEM. **P* < .05, ***P* < .01, and ****P* < .001, by analysis of variance with the Dunn post-test. HSP90, heat shock protein 90.

mediated TGR5 activation was shown to increase BAT thermogenesis.^{20,21} To determine if alcohol-induced BAs work upstream of TGR5 for BAT thermogenesis in AALD, we analyzed the makeup of circulating BAs by liquid chromatography–mass spectrometry. Alcohol consumption significantly increased the circulating levels of unconjugated BAs and taurine-conjugated BAs in WT and TGR5 KO mice (Figure 2A). Interestingly, total serum BA levels were noted to be increased in ethanol-fed mice regardless of genetic background (Figure 2B). Several BAs activate TGR5 to varying degrees.²² To determine whether the alcohol-altered BAs regulate TGR5 activity, we conducted a cell-based reporter assay using the total BAs extracted from the serum of these mice. BAs from ethanol-fed WT and TGR5 KO mice activated TGR5 to the same degree (Figure 2C). These results suggest that ethanol consumption–altered BAs enhance BAT thermogenesis and energy expenditure via activating TGR5 in BAT. Previous studies have shown that alcohol consumption also alters BA biosynthesis and transportation.^{11,12} To test if TGR5 is involved in the regulation of BA biosynthesis and transportation, the expression of BA biosynthesis genes and transporter genes were determined. The results showed that BA biosynthesis genes CYP7A1, CYP7B1, CYP8B1, and CYP27A1 were down-regulated after ethanol feeding in WT and TGR5 KO mice (Figure 2D). Western blot analysis further confirmed the down-regulation of CYP7A1 in the liver (Figure 2E). After ethanol feeding, the expression of sodium/taurocholate cotransporting polypeptide and organic anion transporting polypeptide 1B1, the main transporters that control reabsorption of BAs from the enterohepatic circulation into hepatocytes, also were down-regulated (Figure 2F). The transporter genes *BSEP* and *MRP2*, which are responsible for secreting BAs into the gallbladder, were decreased too. In contrast, after ethanol feeding, the transporters organic solute transporter β and multidrug resistance-associated protein 4, which control the efflux of BAs into portal blood, were strongly up-regulated in both WT and TGR5 KO mice (Figure 2F and G). The regulation of these BA transporters may partly explain the increased circulating BA levels in alcohol-fed WT and TGR5 KO mice. The chronic-plus-one-binge ethanol feeding–induced AALD mouse model faithfully recapitulates the steatosis and liver injury individuals experience with chronic alcohol abuse.¹⁸ To investigate if the BA circulation in human AALD is regulated via a similar mechanism as in mice, we measured these genes in human beings. Consistently, similar changes were observed in BA genes in the liver of AALD patients compared with the non-AALD controls (Figure 2H and I), suggesting that, in the rodent model and human beings, ethanol-mediated variation in circulating BAs are not owing to increased BA biosynthesis, but to altered BA distribution. Our results show that TGR5 was not involved in altering alcohol-induced changes in the BA profile.

TGR5 Deficiency Exacerbates AALD in Mice

To determine how decreased BAT thermogenesis by TGR5 deficiency promotes AALD, we compared the AALD

phenotypes in ethanol-fed WT and TGR5 KO mice. Ethanol-fed mice all showed hepatic steatosis and liver injury, as demarcated by increased serum ALT and aspartate aminotransferase (AST) levels, a higher liver/body weight ratio, and more lipid accumulation and increased inflammatory gene expression in the liver (Figure 3A–E). However, EtOH-KO mice showed a greater degree of pathology, recapitulating the findings of others.²³ Moreover, EtOH-KO mice showed severe liver fibrosis, as shown by Sirius red staining, which was attenuated in WT animals (Figure 3D). Programmed cell death plays a role in the progression of AALD.²⁴ Consistently, there was increased cell death on terminal deoxynucleotidyl transferase–mediated deoxyuridine triphosphate nick-end labeling assay in livers from EtOH-KO mice vs EtOH-WT mice. Expression of cleaved caspase-3, an apoptosis marker, was noted in livers from EtOH-KO mice (Figure 3D). Immunohistochemistry staining on liver sections using cluster of differentiation (CD)68 and F4/80 antibody, respectively, supported that ethanol consumption increased inflammation in the liver, particular with significantly higher numbers of CD68-positive cells in TGR5 KO mice (Figure 3D). Multiple inflammatory genes including *IL1 β* , *IL6*, and *TNF- α* were linked to ethanol-induced hepatocyte death.²⁴ Ethanol feeding significantly increased mRNA levels of *IL1 β* and *IL6* in ethanol-fed TGR5 KO, but not WT, mice (Figure 3E). Male mice showed similar results in this experiment (Figure 3F–I). These results showed that TGR5 deficiency exacerbates alcohol-induced liver steatosis, inflammation, cell death, and fibrosis, suggesting that BA-activated BAT TGR5 plays a key role in preventing the pathogenesis of AALD.

BAT-Specific TGR5 Knockdown Exacerbated AALD in Mice

To determine the critical role of BAT TGR5, we further generated a BAT-specific TGR5 knockdown (TGR5 KD) mouse model using Adeno-associated virus (AAV) 2/9-mediated clustered regularly interspaced palindromic repeats/CRISPR-associated proteins system 13d (Crisper/Cas13d) system containing a mini-UCP1–TGR5 single-guide RNA (sgRNA), and then subjected the mice to alcohol-induced AALD. As shown in Figure 4A and B, the expression of TGR5 was decreased significantly in the BAT, but not other tissues such as liver and intestine of TGR5 KD mice compared with WT mice. Similar changes in thermogenesis genes, UCP1 protein levels, and fatty acid oxidation activity in BAT also were observed in TGR5 KD mice (Figure 4C–E), as observed in TGR5 KO mice (Figures 1 and 5G). Ethanol consumption increased the serum ALT level in both WT and KD mice, whereas TGR5 KD mice showed a significantly higher level than WT mice (Figure 4F). There was significantly more lipid accumulation in ethanol-fed TGR5 KD (EtOH-KD) mice compared with EtOH-WT mice (Figure 4G and H). The ethanol-induced hepatic inflammatory genes also showed a trend of higher levels in EtOH-KD mice (Figure 4I). These results showed that BAT-specific TGR5 KD exacerbated AALD in mice. Together, these results

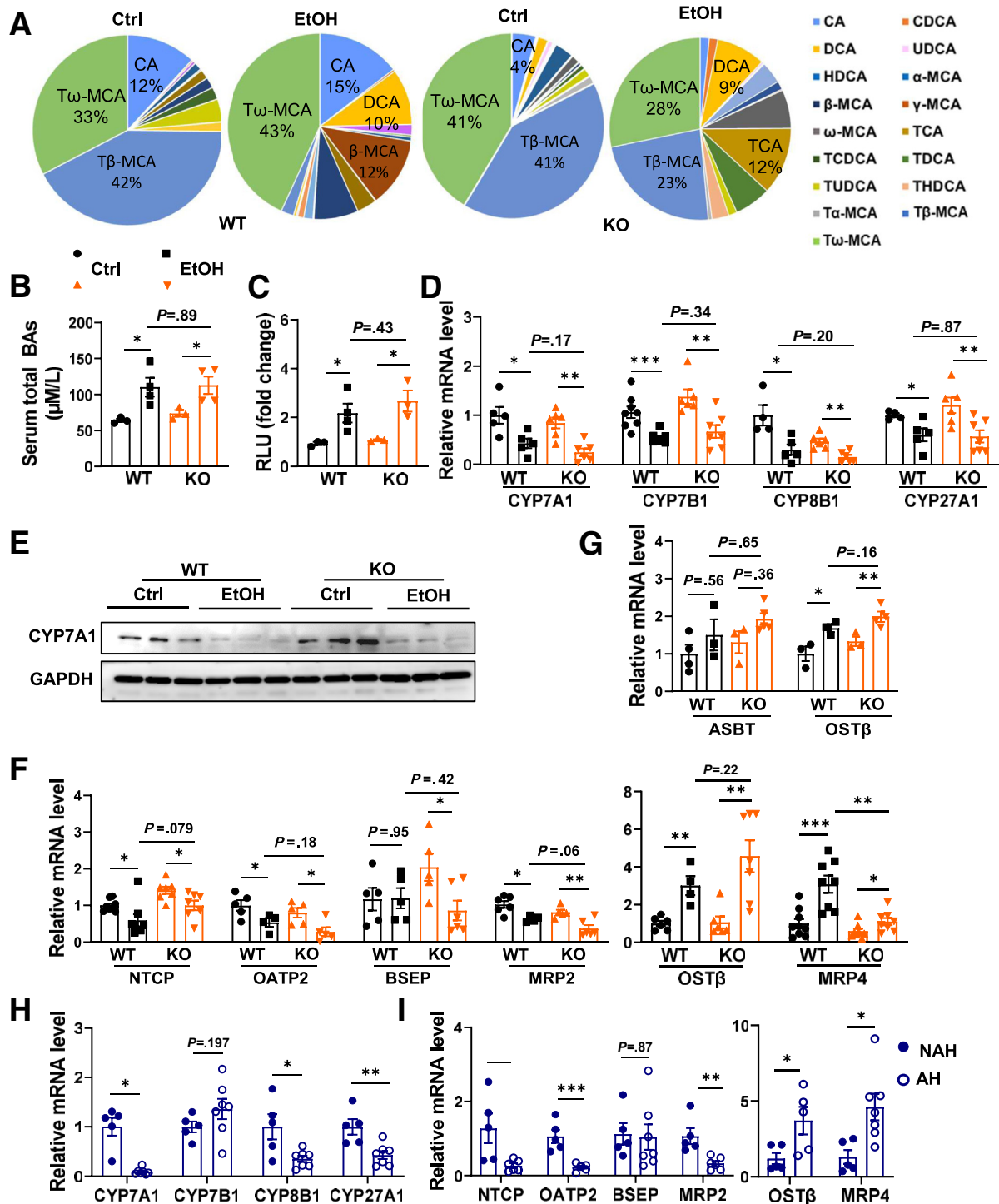


Figure 2. Alcohol-mediated changes in BAs activates TGR5 in BAT. Eight- to 10-week-old female WT and TGR5 KO mice were subjected to chronic-plus-one-binge ethanol feeding to induce AALD. $n = 5-10$ per group. (A) Serum BA profile. $n = 6-8$ per group. (B) Serum total BA levels. (C) Fold induction of relative light unit (RLU) by serum BAs in luciferase assay. (D) Relative mRNA levels of hepatic BA biosynthesis genes. (E) Western blot analysis of CYP7A1 in liver. (F) Relative mRNA levels of BA transporter genes in the liver. (G) Relative mRNA levels of BA transporter genes in distal small bowel (ileum). (H) Relative mRNA levels of BA biosynthesis genes in livers of individuals with AH ($n = 8$) compared with that of non-AH samples (NAH, $n = 5$). (I) Relative mRNA levels of liver transporter genes in livers of individuals with AH ($n = 8$) or individuals with nonalcoholic hepatitis healthy livers (NAH, $n = 5$). Values are means \pm SEM, $*P < .05$, $**P < .01$, and $***P < .001$, by analysis of variance with the (A-F) Dunn post-test or (H and I) unpaired Student t test. ASBT, apical sodium-dependent bile acid transporter; β -MCA, β -Muricholic acid; CA, Cholic acid; CDCA, Chenodeoxycholic acid; Ctrl, control; DCA, Deoxycholic acid; GAPDH, glyceraldehyde-3-phosphate dehydrogenase; HDCA, Hyodeoxycholic acid; OST β , organic solute transporter β ; T β -MCA, Taurine β -Muricholic acid; TCDCA, Taurochenodeoxycholic acid; THDCA, Taurohyodeoxycholic acid Sodium Salt; TUDCA, Tauroursodeoxycholic acid Sodium Salt; T ω -MCA, Taurine ω -Muricholic acid; UDCA, Ursodeoxycholic acid.

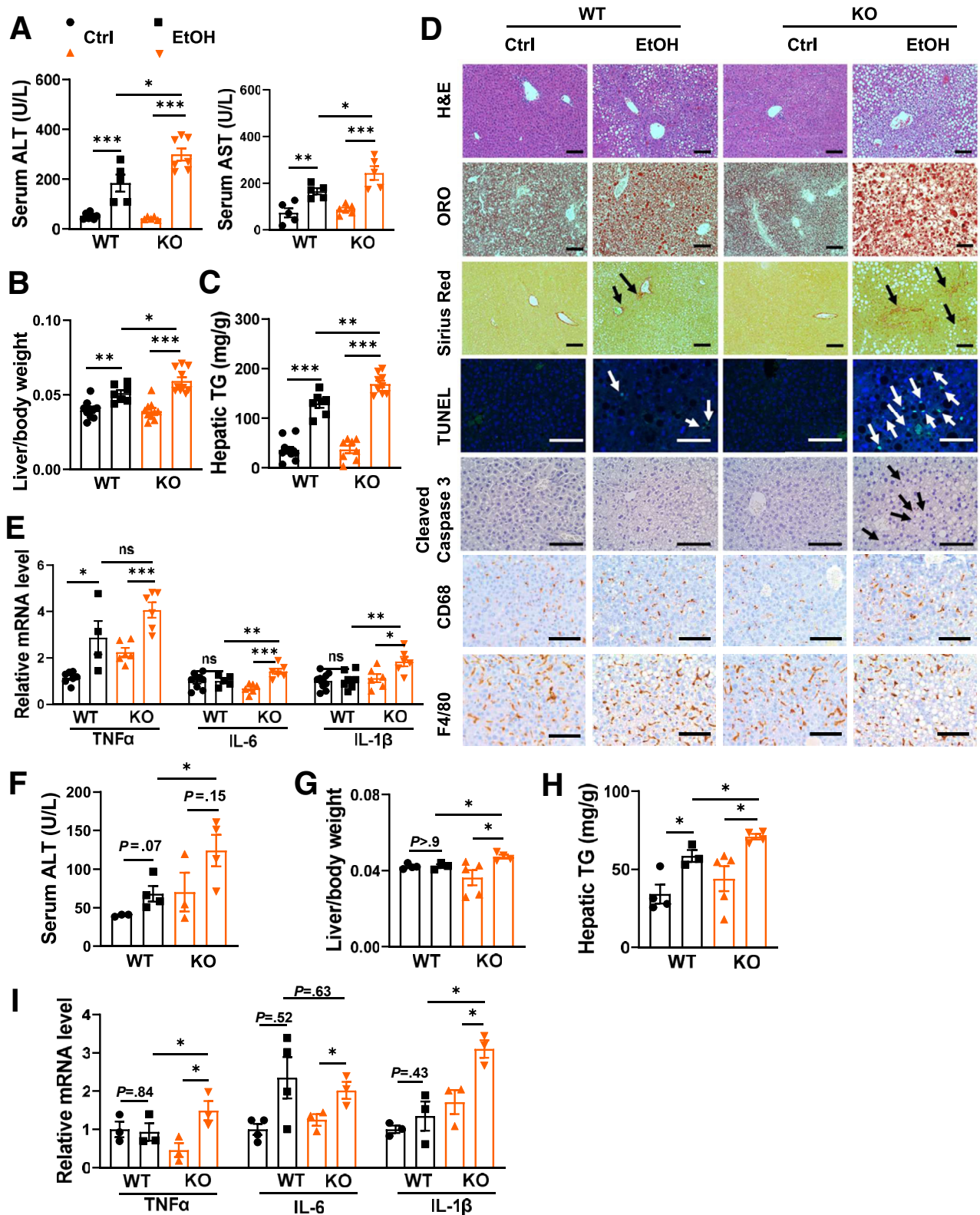


Figure 3. TGR5 deficiency exacerbates AALD in mice. Eight- to 10-week-old (A–E) female or (F–I) male WT and TGR5 (A–E) KO or (F–I) KD mice were subjected to chronic-plus-one-binge ethanol feeding to induce AALD. (A) Serum levels of ALT and aspartate aminotransferase (AST). (B) Liver/body weight ratios. (C) Hepatic triglycerides (TG) levels. (D) Representative images of liver sections stained with the indicated reagents. Scale bars: 100 μ m. (E) Relative mRNA levels of inflammatory genes in liver. $n = 5$ –10 per group. (F) Serum levels of ALT in male mice. (G) Liver/body weight ratios in male mice. (H) Hepatic TG levels in male mice. (I) Relative mRNA level of inflammatory genes in liver in male mice. $n = 3$ –5 per group. Values are means \pm SEM. * $P < .05$, ** $P < .01$, and *** $P < .001$, by analysis of variance with the Dunn post-test. Ctrl, control; ORO, Oil red O; TUNEL, terminal deoxynucleotidyl transferase–mediated deoxyuridine triphosphate nick-end labeling.

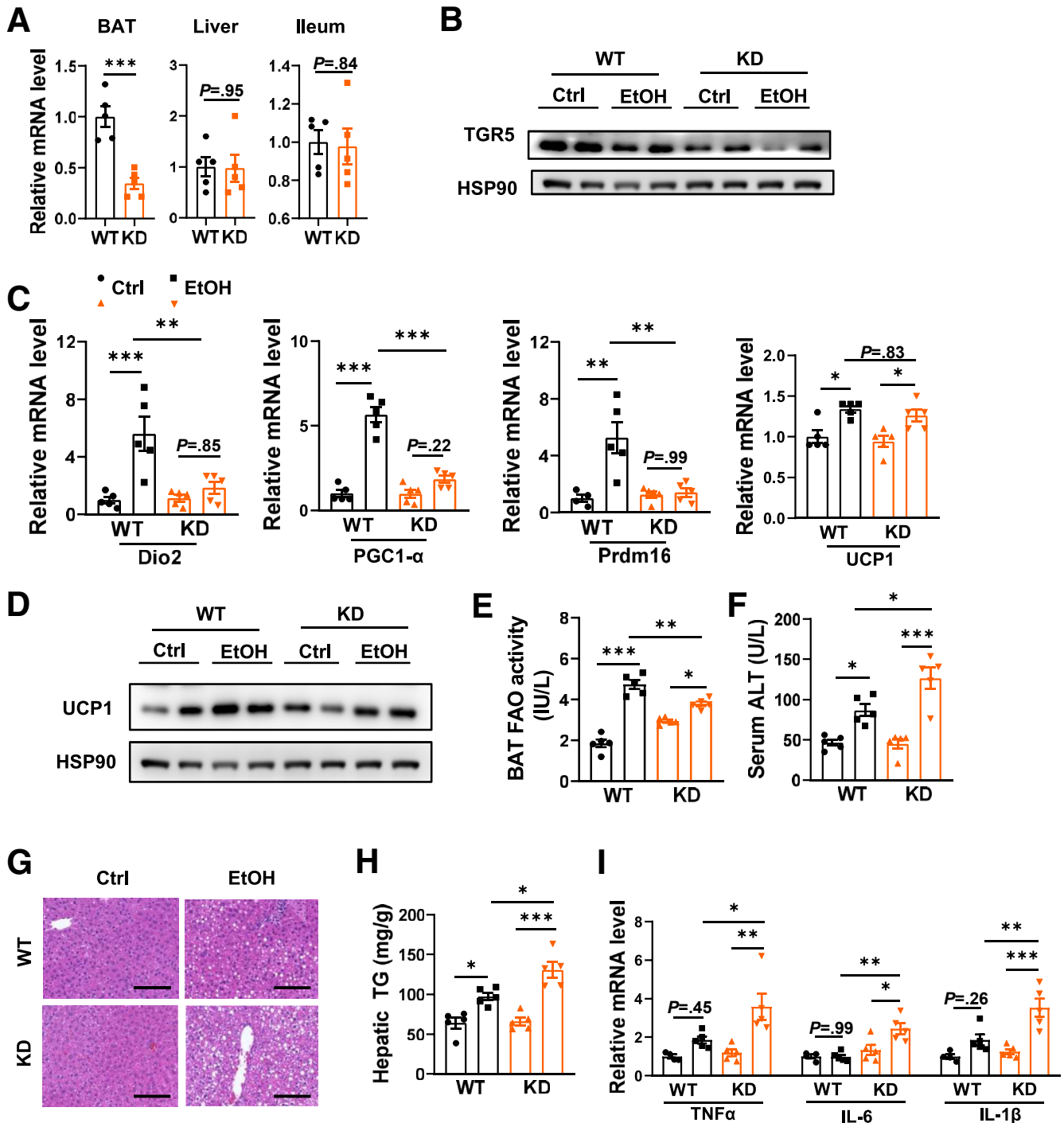


Figure 4. BAT-specific TGR5 knockdown exacerbated AALD. Eight to 10-week-old BAT-specific TGR5 KD female mice and their WT control mice were subjected to chronic-plus-one-binge ethanol feeding to induce AALD. (A) Relative mRNA levels of TGR5 in BAT, liver, and ileum. (B) Western blot analysis of TGR5 in BAT. (C) Relative mRNA levels of thermogenesis genes in BAT. (D) Western blot analysis of UCP1 in BAT. (E) Fatty acid oxidation (FAO) activity in BAT. (F) Serum ALT levels. (G) Representative images of H&E-stained liver sections. Scale bar: 100 μ m. (H) Hepatic TG. (I) Relative mRNA levels of inflammatory genes in liver. $n = 5$ per group. Values are means \pm SEM. * $P < .05$, ** $P < .01$, and *** $P < .001$, by analysis of variance with the Dunn post-test. Ctrl, control; HSP90, heat shock protein 90.

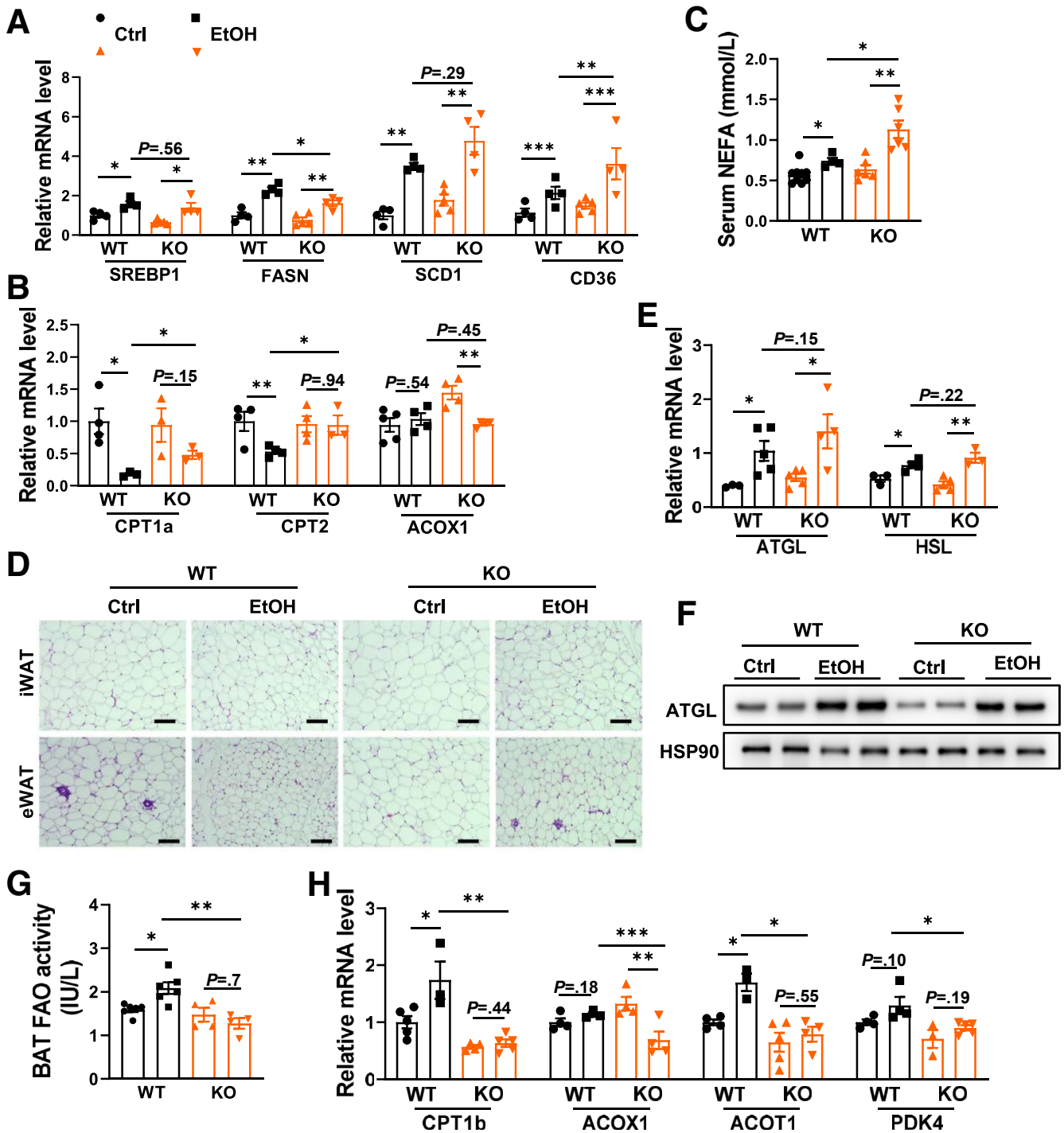


Figure 5. TRG5 deficiency enhances adipose tissue FFA release and liver uptake to worsen steatosis. Eight- to 10-week-old female WT and TGR5 KO mice were subjected to chronic-plus-one-binge ethanol feeding to induce AALD. (A) Relative mRNA levels of genes involved in lipogenesis and FFA uptake in liver. (B) Relative mRNA levels of genes involved in hepatic β -oxidation. (C) Serum NEFA levels. (D) Representative images of H&E-stained inguinal (iWAT) and epididymal (eWAT) adipose tissue sections. Scale bars: 100 μ m. (E) Relative mRNA levels of genes involved in lipolysis in iWAT. (F) Protein levels of adipose triglyceride lipase (ATGL) in iWAT. (G) Fatty acid oxidation (FAO) activity in BAT. (H) Relative mRNA levels of genes involved in β -oxidation in BAT ($n = 4-6$ per group). Values are means \pm SEM. * $P < .05$, ** $P < .01$, and *** $P < .001$, by analysis of variance with the Dunn post-test. Ctrl, control; HSP90, heat shock protein 90.

further confirm a critical role of BAT TGR5 in the development of AALD.

TGR5 Deficiency Induces Adipose Tissue Free Fatty Acid Release and Liver Uptake to Worsen Steatosis

In the present study, ethanol and food intake were comparable between WT and KO mice, mitigating the effects of diet on variation in hepatic-derived lipids.²⁵ Still, de novo lipogenesis is an important contributor to increased lipid accumulation.^{2,26} Here, too, no significant difference in de novo lipogenesis was appreciated between EtOH-KO and EtOH-WT mice (Figure 5A), suggesting that TGR5 deficiency does not cause more de novo lipogenesis in these animals. mRNA levels of the free fatty acid (FFA) β -oxidation-associated genes *CPT1a*, *CPT2*, and *ACOX1* were comparable in both treatment groups (Figure 5B), suggesting that TGR5 deficiency did not suppress FFA β -oxidation in the liver. Interestingly, levels of serum nonesterified FFA (NEFA) were increased in EtOH-KO compared with EtOH-WT mice (Figure 5C). Relative to its role in FFA uptake, hepatic CD36 mRNA was increased in livers from EtOH-KO mice (Figure 5A). Alcohol exposure activates adipocyte lipolysis and increases FFA release,^{27,28} while TGR5 is involved in adipocyte lipolysis.²⁹ Adipocytes in white adipose tissue (WAT) were noted to be smaller in both WT and TGR5 mice after ethanol feeding (Figure 5D). Along with this, several genes that regulate adipocyte lipolysis in WAT, including *ATGL* and *HSL*, were increased in EtOH-KO and EtOH-WT mice (Figure 5E and F), suggesting that TGR5 deficiency did not significantly affect adipocyte lipolysis. Lastly, fatty acid oxidation activity was up-regulated significantly in BAT of WT, but not TGR5 KO, mice (Figure 5G), and genes involved in FFA β -oxidation were decreased significantly in BAT from EtOH-KO mice compared with EtOH-WT mice (Figure 5H), suggesting that TGR5 deficiency reduces FFA β -oxidation in BAT.

TGR5-Mediated BAT Thermogenesis Is Independent of Temperature in AALD

Cold activates thermogenesis to maintain a stable core body temperature whereas increasing ambient temperature leads to BAT inactivation.³⁰ At thermoneutrality (30°C), BAT became inactive, and was associated with enlarged lipid droplets and inhibited UCP1 expression, whereas ethanol consumption reverses these changes in mice,¹⁸ suggesting that, in AALD, BAT preferentially may participate in heat generation independent of cold-induced thermogenesis. To test this, WT and KO mice were housed at 30°C for 2 weeks and then given ethanol as described.^{11,18} Similar to results in mice housed at 22°C (Figure 1), WT and KO ethanol-fed mice at a thermal neutral temperature of 30°C showed increases in several parameters including ALT levels, liver/body weight ratios, hepatic triglyceride levels, serum NEFA levels (Figure 6A), and liver lipid accumulation (Figure 6B). Again, these changes were exaggerated in KO vs WT mice. Thermogenesis-associated genes including *Dio2*, *PGC1- α* , *Ucp1*, and *Prdm-16*, as well as UCP1 protein levels, tracked

along with those noted in mice housed at 22°C (Figure 6C and D). As a result of suppressed thermogenesis at 30°C, lipid droplets were more prominent in BAT from WT and TGR5 KO control mice compared with animals housed at 22°C. Importantly, under a thermal neutral environment, ethanol feeding markedly reduced lipid accumulation in BAT from WT, but not TGR5 KO, mice (Figure 6E). These results show that TGR5-mediated BAT thermogenesis in AALD is independent of temperature, suggesting that BAs play an independent role in stimulating alcohol-induced fat burning and energy expenditure.

Treatment With the TGR5-Specific Agonist 23(S)-Methyl-Lithocholic Acid Promotes BAT Activation and Ameliorates AALD

Our results suggest that TGR5 plays a protective role against AALD. No changes in murine liver or BAT TGR5 expression were found with ethanol feeding (Figure 7A), supporting the idea that targeting TGR5 may lessen AALD. We developed a selective potent agonist, 23(S)-methyl-lithocholic acid (DY284), of TGR5.³¹ WT and TGR5 KO mice were treated with DY284 (30 mg/kg) by oral gavage once daily from the beginning of ethanol feeding to the end of the experiment.³¹ The serum and hepatic BA concentration was not altered significantly with DY284 treatment (Figure 7B and C). DY284 treatment significantly decreased ALT levels (Figure 7D), expression of hepatic inflammatory genes (Figure 7E), the liver/body weight ratios (Figure 7F), and hepatic and serum triglyceride levels (Figure 7G and H) in WT mice. H&E staining showed less liver lipid accumulation in WT mice treated with DY284 (Figure 7I). However, there were no significant differences in these therapeutic phenotypes in TGR5 KO mice. Expression of TGR5 downstream thermogenesis genes (Figure 7J), UCP1 protein (Figure 7K), and FFA β -oxidation genes (Figure 7L) all were increased significantly in BAT of WT mice, suggesting the activated BAT by TGR5 agonist. Consequently, the serum levels of NEFA were decreased in WT, but not TGR5 KO, mice after DY284 treatment (Figure 7M). These results suggest that activating BAT thermogenesis by TGR5 agonist can protect the development of AALD.

Discussion

BA circulation and signaling are closely associated with the development of AALD. In this regard, CYP7A1¹¹ and FXR¹² deficiency exacerbates AALD, indicating the importance of maintaining BA homeostasis under these conditions. Chronic alcohol consumption increases circulating BA levels in human beings and rodents.⁷⁻¹⁰ We found that chronic alcohol consumption reduced expression of key BA synthesis genes. Interestingly, we also found that ethanol decreased expression of BA transporters that control BA intake from the portal vein, but increased expression of BA transporters that control BA efflux from enterohepatic circulation to blood circulation in human beings and rodents. Together, these changes could, in part, explain alcohol-mediated increases in circulating BAs. BA signaling is known to regulate metabolism, yet it is not clear how BAs

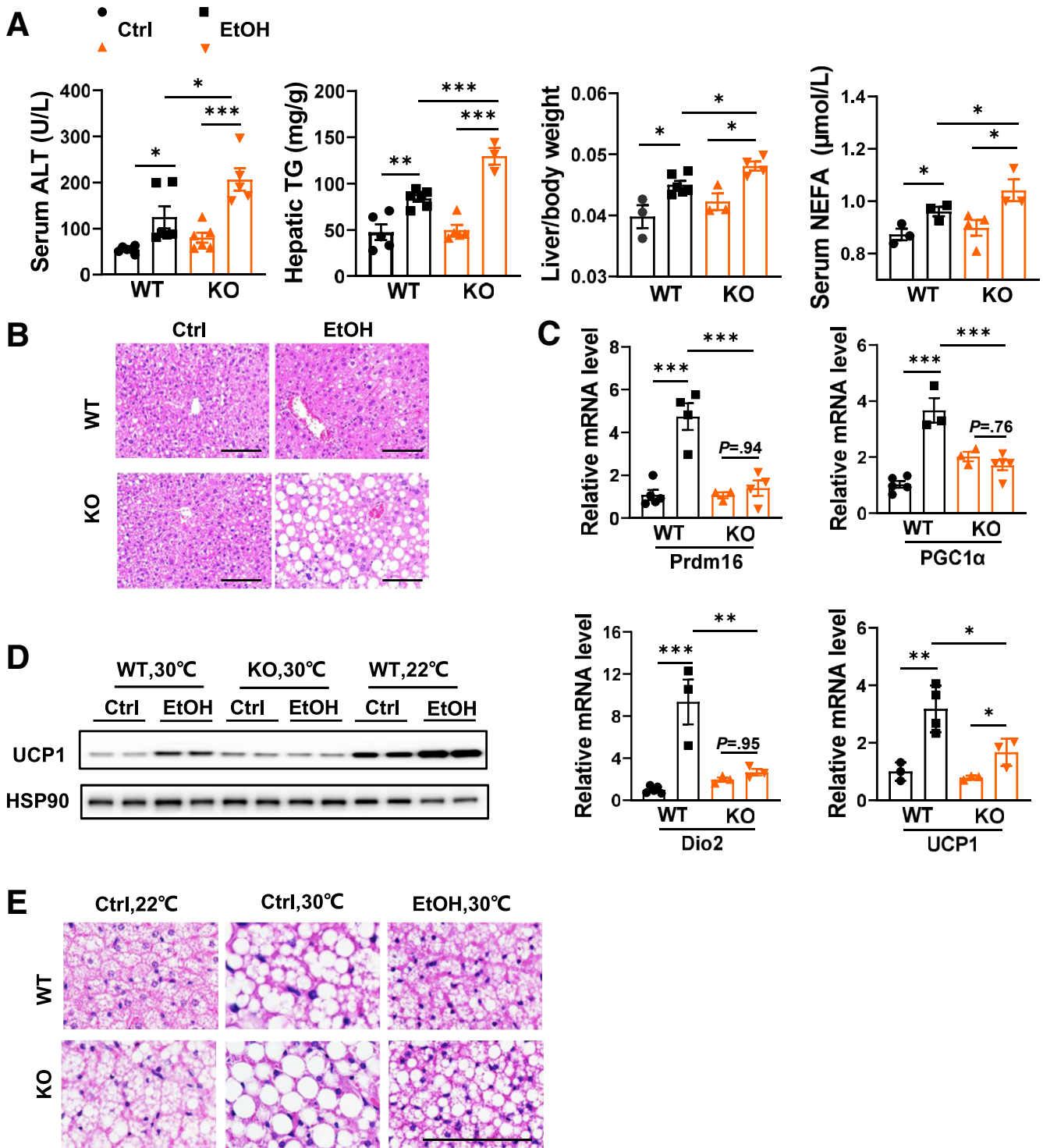


Figure 6. TGR5-mediated BAT thermogenesis is independent of temperature in AALD. Eight- to 10-week-old female WT and TGR5 KO mice were placed in a 30°C chamber for 2 weeks and then given chronic-plus-one-binge ethanol feeding to induce AALD. (A) Parameters of AALD phenotype in mice, including liver/body weight ratios, hepatic triglycerides (TG), serum NEFA, and ALT levels. (B) Representative images of H&E-stained liver tissue sections. Scale bars: 100 μ m. (C) Relative mRNA levels of thermogenesis genes in BAT. (D) Protein levels of UCP1 in BAT. (E) Representative images of H&E-stained BAT tissue sections. Scale bars: 100 μ m. $n = 4-5$ per group. Values are means \pm SEM. * $P < .05$, ** $P < .01$, and *** $P < .001$, by analysis of variance (ANOVA) with the Dunn post-test. Ctrl, control; HSP90, heat shock protein 90.

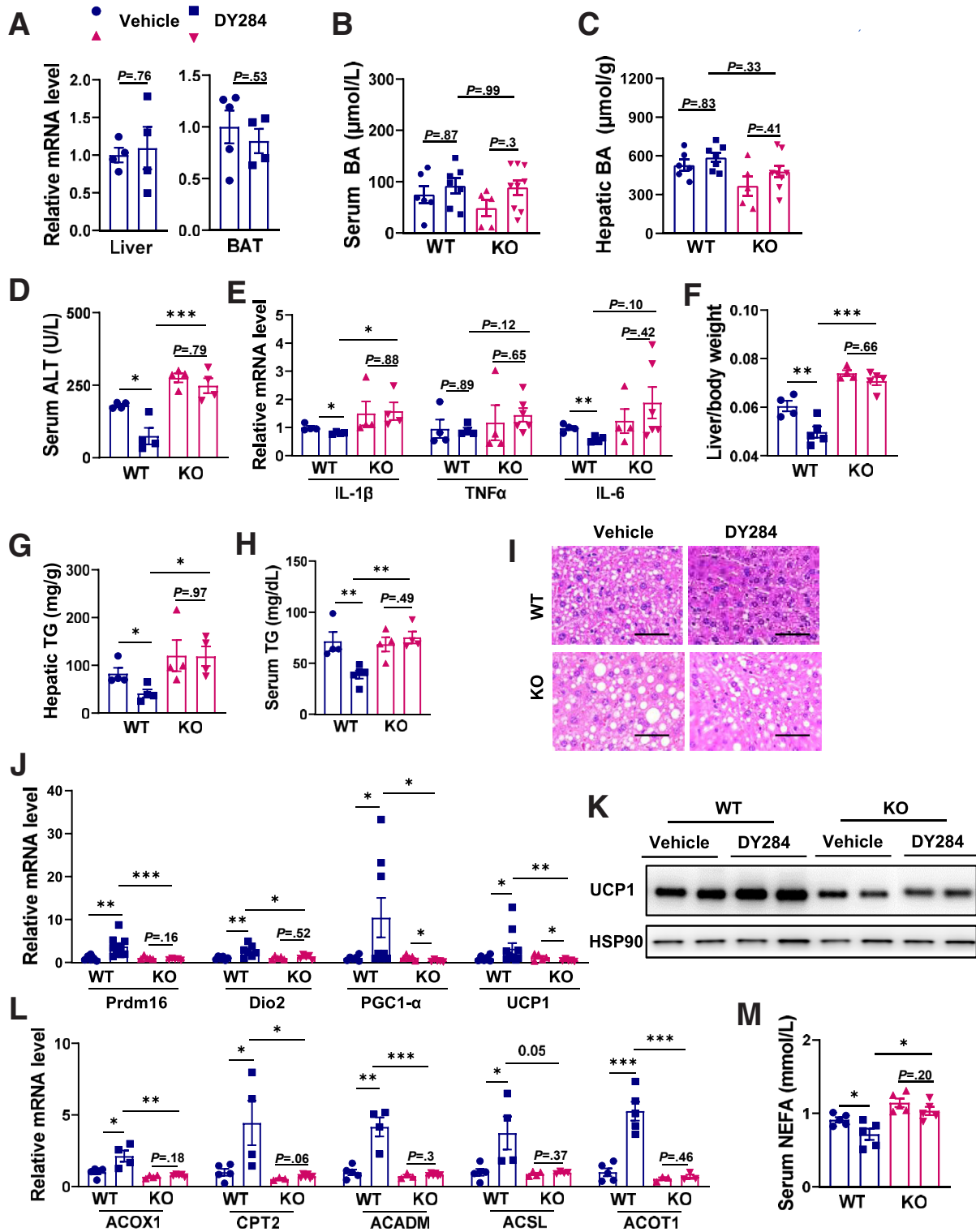


Figure 7. Treatment with the TGR5-specific agonist DY284 promotes BAT activation and ameliorates AALD. Eight- to 10-week-old female WT and TGR5 KO mice were subjected to chronic-plus-one-binge ethanol feeding to induce AALD. DY284 was administered at 30 mg/kg to mice by oral gavage once daily from the 1st to the 16th day. (A) Relative mRNA levels of TGR5 in the liver and BAT. (B) Serum BA concentration. $n = 5-9$ per group. (C) Hepatic BA concentration. $n = 4-6$ per group. (D) Serum ALT levels. (E) Relative mRNA levels of inflammatory genes in the livers from mice. (F) Liver/body weight ratios. (G) Hepatic triglycerides (TG) levels. (H) Serum TG levels. (I) Representative images of H&E-stained liver and BAT tissue sections. Scale bars: 200 μm . (J) Relative mRNA levels of genes involved in BAT thermogenesis. (K) Protein levels of UCP1. (L) Relative mRNA level of genes involved in BAT β -oxidation. (M) Serum NEFA levels. $n = 4-6$ per group. Values are means \pm SEM. $*P < .05$, $**P < .01$, and $***P < .001$, by (A and C) unpaired Student t test or analysis of variance with the (D-M) Dunn post-test. HSP90, heat shock protein 90.

regulate the development of AALD. As a nuclear BA receptor, FXR protects the liver from AALD by maintaining BA homeostasis and the enterohepatic BA circulation.¹² TGR5 is a membrane BA receptor.³² Expanding on this, we showed that TGR5 deficiency did not affect alcohol-mediated effects on BA synthesis and transportation in mice. Rather, we discovered that an alcohol-induced increase of BAs in circulation activates TGR5 in BAT to regulate fatty acid metabolism, providing a new mechanism for the role of BA signaling in the development of AALD. Reported evidence also has shown that compared with healthy controls, AALD patients had higher levels of BAs that are endogenous TGR5 agonists, including Lithocholic acid (LCA), Chenodeoxycholic acid (CDCA), and Cholic acid (CA), as well as their glycine- and taurine-conjugated BAs,^{22,33} suggesting that alcohol consumption-altered BAs may activate TGR5 in human beings.

The contribution of adipose tissues to AALD has been recognized previously, which is receiving more attention recently because of the current global epidemic of obesity.^{34,35} Alcohol causes WAT dysfunction by increasing lipolysis and adipocyte death, which leads to pathologic release of FFAs and inflammatory mediators.³⁶ In contrast, although alcohol has been known to increase the mass and oxidative capacity of BAT dozens of years ago,^{37,38} the role of BAT in the development of AALD still is unclear. Yoshimoto et al³⁹ observed that intraperitoneal injection of ethanol induced UCP1 mRNA expression in BAT. Similarly, deletion of *Ucp1* in BAT in mice worsened AALD putatively through blocking of *Ucp1*-mediated thermogenesis and increasing liver lipids.¹⁸ This study thus shows an important role of BAT in protecting against the development of AALD. However, the mechanism driving BAT thermogenesis during AALD remains largely unknown. The present study identified a new mechanism by which BAs enhanced BAT TGR5 activity to protect the liver from AALD. More broadly, TGR5 deficiency did not alter alcohol-stimulated adipose lipolysis, de novo hepatic lipogenesis, or alcohol effects on hepatic FFA β -oxidation. This is relevant because alcohol stimulates release of FFAs from WAT and increases liver uptake of FFAs, thereby promoting liver steatosis and AALD. Our results show that TGR5 deficiency significantly suppressed BAT thermogenesis and reduced FFA oxidation, leading to increased circulating FFAs and hepatic uptake of FFAs and lipid accumulation in AALD. Moreover, thermoneutral experiments indicated that TGR5 is required for BAT fat burning, independent of temperature-induced thermogenesis. These results thus suggest that BA/TGR5-mediated BAT activation after alcohol consumption plays a protective role against AALD.

TGR5 is a key player of several metabolic pathways, including energy homeostasis, glucose metabolism, and hepatic inflammation; thus, it has been broadly used as a target for drug discovery to treat type 2 diabetes, steatohepatitis, obesity, and atherosclerosis.⁴⁰ However, limited information is available for AALD drug development by targeting TGR5. Iracheta-Vellve et al⁴¹ speculated that TGR5 agonist may ameliorate AALD by suppressing hepatic lipogenic gene expression and inhibiting inflammation signaling

pathways. They were limited with unclear mechanism in regulating these genes and uncertain target using a WT mouse model. More recently, Spatz et al²³ made a point that TGR5 deficiency induced gut microbiota dysbiosis, which is independent of alcohol intake, contributing to the worsened alcohol-induced liver inflammation. They provided evidence that TGR5 is involved in reshaping the gut microbiota profile, linking TGR5 with AALD development, which can be supported by the well-known roles of gut microbiota in AALD.⁴² Our results show that BA-mediated BAT thermogenesis plays a critical role in AALD, suggesting that enhancing BAT function via TGR5 activation is a potential therapeutic approach for the treatment of AALD. This is confirmed further by our investigation that the specific TGR5 agonist DY284 activates BAT and efficaciously ameliorates alcohol-induced steatosis and liver injury in WT, but not TGR5 KO, mice. Our study provides convincing evidence to support the promising target role of BAT TGR5 for the treatment of AALD. Considering the important roles of TGR5 in other tissues such as liver and intestine, future work in tissue-specific evaluation will help determine the role of TGR5 in these tissues in mediating AALD development, and will be helpful for a full pharmacologic characterization of TGR5 agonists in the treatment of AALD in an even broader context.

In conclusion, our results show that the alcohol altered BA distribution in circulation, which executes their effects on AALD by activating TGR5 signaling in BAT. TGR5 plays a protective role against AALD through enhancing BAT

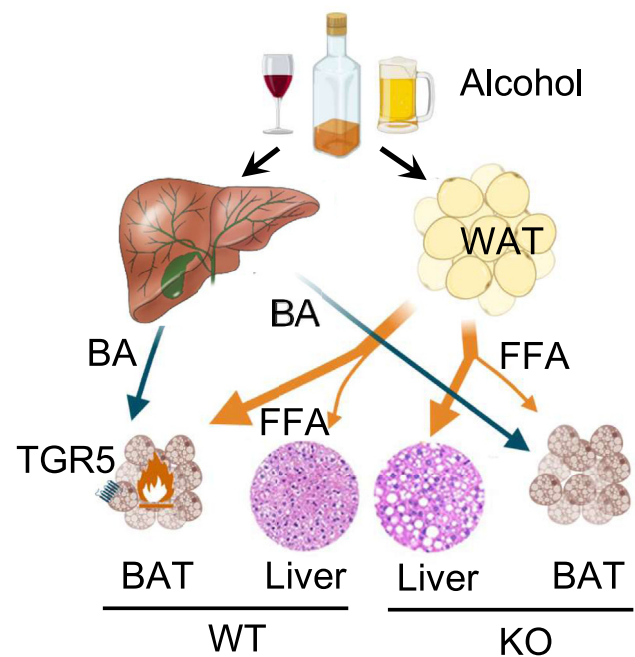


Figure 8. BA-mediated activation of BAT TGR5 protects liver from AALD. Alcohol altered the BA distribution toward increased levels in the circulation and to stimulate white adipocyte lipolysis to release FFAs. Altered BAs activate TGR5-mediated FFA β -oxidation and thermogenesis in BAT, leading to decreased hepatic FFA uptake, and thus protecting from AALD.

thermogenesis and reducing FFA release and hepatic FFA uptake (Figure 8). These findings further support a critical role for BAT in protection against the development of AALD and provide evidence that BA-mediated BAT activation via TGR5 is behind this protection.

Materials and Methods

Animals

TGR5 KO mice on a C57BL/6J background were kindly provided by Dr Vassileva Galya at Merck & Co.⁴³ All animal procedures were approved by the City of Hope Institutional Animal Care and Use Committee (protocol 19029) and conducted in accordance with the National Institutes of Health Guidelines for the Care and Use of Laboratory Animals. Mice were housed in a 12-hour light/dark cycle in a temperature-controlled room (25°C) with a relative humidity of 50%. To induce AALD, 8- to 10-week-old wild-type C57BL/6J (WT) and TGR5 KO mice underwent chronic-plus-one-binge ethanol feeding as described.^{11,18} Mice were fed a control liquid diet (F1259SP, Lieber-Decarli'82; Bio-Serv, Flemington, NJ) for the first 5 days, and then fed a liquid diet with 5% (vol/vol) ethanol (Pure + Denatured, 2701; Dencon Labs, King of Prussia, PA) for 10 days. On day 16, mice were orally gavaged with a single binge dose of isocaloric ethanol (5 g/kg body weight). A control liquid diet and the final binge with maltose dextrin (10 DE; Food Grade, Flemington, NJ) gavage was used for the control groups. The TGR5 agonist DY284 [23[S]-methyl-Lithocholic acid (LCA) (homemade), was administered at 30 mg/kg to mice once daily from the 1st to the 16th day by oral gavage. All mice

were killed humanely in accordance with City of Hope animal resources protocols 9 hours after binge.

Human AH Samples

All procedures that involved human AH sample collection were approved by the Ethics Committee of Institutional Review Boards at Johns Hopkins Medical Institutions and conformed to the ethical guidelines of the 1975 Declaration of Helsinki. Written informed consent was signed by all individuals or their families. Liver tissues were excised from explanted livers in patients with severe AH during liver transplantation, or wedge biopsy specimens from the healthy donor livers as described previously.⁴⁴ Samples were diagnosed by histologic review and individuals' blood biochemical indicators (Table 1). No donor organs were obtained from executed prisoners or other institutionalized individuals.

Metabolic Parameter Measurements

Serum ALT and aspartate aminotransferase levels were measured using the EnzyChrom Alanine Transaminase Assay Kit (EALT100; Bioassay, Hayward, CA) and the EnzyChrom Aspartate Transaminase Assay Kit (EASTR-100; Bioassay). Serum levels of NEFA were measured using a NEFA Assay kit (TK036; Wako, Neuss, Germany). Hepatic triglyceride levels were measured using the L-Type Triglycerides M Kit (TK006; Wako). Total serum BAs were measured using the Diazyme TBA Assay kit (DZ042A-K; DIAZYME, Poway, CA).

Table 1. Characteristics of AH Patients

AH ID	Age, y	Sex	AST, U/L	ALT, U/L	ALB, g/dL	TBIL, mg/dL	WBC, $\times 10^3/\mu\text{L}$	HB, g/dL	PLT, K/cu mm	DCM
51	50	F	55	14	4.2	39.9	13.37	7.7	102	Acute on chronic hepatitis
52	48	F	158	86	3.8	28	28.91	10.3	158	Acute on chronic hepatitis
53	47	M	97	36	2.6	28.5	29.59	7.2	31	Acute on chronic hepatitis
54	39	F	62	30	4.2	24.9	17.06	6.9	95	Acute hepatitis
55	60	M	115	44	2.3	9.1	14.66	7	41	Acute on chronic hepatitis
56	47	F	23	10	3.3	3.4	8.18	7.3	114	Acute on chronic hepatitis
57	54	F	56	22	3.1	8.2	13.18	8.1	163	Alcoholic cirrhosis and hepatitis
58	58	M	70	32	2.6	4.4	6.51	10.9	84	Alcoholic cirrhosis and hepatitis
	MELD	Creatine	BMI	Steroids pretransplant		Days on steroids pretransplant		Antibiotics		
51	38	2.4	28.6			7		No		
52	36	4.3	34.9	Prednisolone		7		cefepime, vancomycin		
53	32	1.5	28.7	Prednisolone		7		Ceftriaxone		
54	32	1.8	26.5	Prednisolone		35		Ceftriaxone		
55	26	1.6	31.4	Methylprednisone				Ciprofloxacin HCl		
56	27	3.7	24.6	No				Neomycin-polymyxin B-Hydrocortisone		
57	33	3.8	21.6	No				Sulfamethoxazole-trimethoprim		
58	27	3.3	29.3	No				Cefepime, vancomycin		

ALB, albumin; AST, aspartate aminotransferase; BMI, body mass index; DCM, decompensation; HB, hemoglobin; MELD, model for end-stage liver disease score; PLT, platelet; TBIL, total bilirubin; WBC, white blood cell.

Staining of Liver and Adipose Tissue Sections

Liver and adipose tissues were fixed in 4% formalin and embedded in optimal cutting temperature compound or paraffin. Oil red O staining or H&E staining was performed as described previously.⁴⁵ The terminal deoxynucleotidyl transferase-mediated deoxyuridine triphosphate nick-end labeling assay was performed using an In-Situ Cell Death Detection Fluorescein kit (11684795910; Roche, St. Louis MO). Sirius red staining

was performed using Picro Sirius Red Solution (ab246832; Abcam, Cambridge, MA). For immunostaining, sections were incubated with a rabbit anti-cleaved caspase-3 antibody (Asp175, 5A1E; Cell Signaling Technology, Danvers, MA) or UCP1 (10983; Abcam) overnight at 4°C and then incubated with a horseradish-peroxidase-conjugated secondary antibody using a mouse- and rabbit-specific horseradish-peroxidase/3,3'-diaminobenzidine tetra hydrochloride immunohistochemistry detection kit

Table 2. Sequences of Primers for Quantitative PCR

Primer	Forward primer (5'-3')	Reverse primer (5'-3')
Mouse		
CYP8B1	CCTCTGGACAAGGGTTTTGTG	GCACCGTGAAGACATCCCC
CYP7A1	GGGATTGCTGTGGTAGTGAGC	GGTATGGAATCAACCCGTTGTC
CYP7B1	GGAGCCACGACCCCTAGATG	TGCCAAGATAAGGAAGCCAAC
CYP27A1	CCAGGCACAGGAGAGTACG	GGGCAAGTGCAGCACATAG
PGC1 α	TATGGAGTGACATAGAGTGTGCT	CCACTTCAATCCACCCAGAAAG
DIO2	AATTATGCCTCGGAGAAGACCG	GGCAGTTGCCTAGTAAAGGT
Prdm16	CCAAGCAAGGGCGAAGAA	AGTCTGGTGGGATTGGAATGT
UCP1	AGGCTTCCAGTACCATTAGGT	CTGAGTGAGGCAAAGCTGATTT
CPT1a	CTCCGCCTGAGCCATGAAG	CACCAGTGATGATGCCATTCT
CPT1b	GCACACCAGGCAGTAGCTTT	CAGGAGTTGATTCCAGACAGGTA
CPT2	CAGCACAGCATCGTACCCA	TCCAATGCCGTTCTCAAAT
ACOX1	TAACCTCCTCACTCGAAGCCA	AGTTCATGACCCATCTCTGTC
ACOT1	ATACCCCTGTGACTATCCTGA	CAAACACTCACTCAACACTGT
ACADM	AGGGTTTAGTTTTGAGTTGACGG	CCCCGCTTTTGTGATATCCG
ACSL1	TGCCAGAGCTGATTGACATTC	GGCATAACCAGAAGGTGGTGAG
PDK4	AGGGAGGTCGAGCTGTTCTC	GGAGTGTTCACTAAGCGGTCA
NTCP	CAAACCTCAGAAGGACCAACA	TAGGAGGATTATCCCGTTGTG
OATP2	TGAAGCGTTTTTGTCCCTCT	CGGGTGTGGAACATCCCATAA
MRP2	GTGTGGATTCCCTGGGCTTT	CACAACGAACACCTGCTTGG
BSEP	TCTGACTCAGTGATCTTCGCA	CCCATAAACATCAGCCAGTTGT
OST β	GTATTTTCGTGCAGAAGATGCG	TTTCTGTTTCCAGGATGCTC
MRP4	AGGAGCTTCAACGGTACTGG	GCCTTTGTAAAGGAGGGCTTC
ASBT	GTCTGTCCCCCAATGCAACT	CACCCCATAGAAAACATCACCA
TNF- α	TAGTCCTTCTACCCCAATTTCC	TTGGTCCTTAGCCACTCCTTC
IL6	TAGTCCTTCTACCCCAATTTCC	TTGGTCCTTAGCCACTCCTTC
IL1 β	GCAACTGTTCCGTAACCTCAACT	ATCTTTTGGGTCCTCAACT
ATGL	GGATGGCGGCATTTGAGAC	CAAAGGGTTGGGTTGGTTGAG
HSL	GAGACTGGCATCAGTGTGAC	TTGCTAGAGACGATAGCACCT
SREBP1	TGACCCGGCTATTCGGTGA	CTGGGCTGAGCAATACAGTTC
SCD1	TTCTTGCGATACACTCTGGTGC	CGGGATTGAGTGTCTTGTGCT
F	GGAGGTGGTGATAGCCGGTAT	TGGGTAATCCATAGAGCCCAG
CD36	ATGGGCTGTGATCGAACTG	GTCTTCCAATAAGCATGTCTCC
36B4	AACATGCTCAACATCTCCCC	CCGACTCCTCCGACTCTTC
Human		
CYP8B1	GAAGCGCATGAGGACCAAG	TTGCATATTGCCCAAAGTCTAGT
CYP7A1	GAGAAGGCCAAACGGGTGAAC	GGATTGGCACCAAATTGCAGA
CYP7B1	AAAGGTTGGCTTCTTATCTTGG	GCAACTGACTGATGCTAAATGCT
CYP27A1	CGGCAACGGAGCTTAGAGG	GGCATAGCCTTGAACGAACAG
NTCP	AAGGACAAGGTGCCCTATAAAGG	TTGAGGACGATCCCTATGGTG
OATP2	TCCGTCTTCGGCAACATTAAG	GACTTTGAAGTAGGCGCTGTA
MRP2	CCCTGCTGTTGATATACCAATC	TCGAGAGAATCCAGAATAGGGAC
BSEP	TTGGCTGATGTTTGTGGGAAG	CCAAAATGAGTAGCACGCCT
OST β	CAGGAGCTGCTGGAAGAGAT	GACCATGCTTATAATGACCACCA
MRP4	AGCTGAGAATGACGCACAGAA	ATATGGGCTGGATTACTTTGGC
TGR5	GACTTTGACCATGAAGACCAG	GCCCAGACGGAAGTTTCTTATT

ACADM, Acyl-CoA Dehydrogenase Medium Chain; ACOT1, acyl-CoA thioesterase 1; ACOX1, peroxisomal acyl-coenzyme A oxidase 1; ACSL1, Acyl-CoA Synthetase Long Chain Family Member 1; ASBT, apical sodium-dependent bile acid transporter; ATGL, adipose triglyceride lipase; BSEP, bile salt export pump; CPT, carnitine palmitoyltransferase; FASN, Fatty Acid Synthase; HSL, hormone-sensitive lipase; MRP, multidrug resistance-associated protein; NTCP, sodium/taurocholate cotransporting polypeptide; OATP2, organic anion transporting polypeptide 1B1; OST β , organic solute transporter β ; PDK4, pyruvate dehydrogenase lipoamide kinase isozyme 4; PGC1 α , peroxisome proliferator-activated receptor γ coactivator 1 α ; Prdm16, PR domain containing 16; SCD1, stearoyl-CoA desaturase 1; SREBP1, Sterol-regulatory element binding protein 1.

micropolymer (ab236466; Abcam). Hematoxylin was used for the counterstaining of nuclei.

Bile Acid Profile Analysis

Serum bile acid composition was analyzed by liquid chromatography–mass spectrometry as described.⁴⁵

Luciferase Assay

Luciferase assays were performed as described.⁴⁶ HEK 293 cells (ATCC, Manassas, VA) maintained in Dulbecco's modified Eagle medium containing 10% (wt/vol) fetal bovine serum were transiently transfected using polyethylenimine (Promega, Madison, WI) and allocated to 24-well plates 16 hours before transfection. Cells were transfected with plasmids encoding full-length TGR5 and plasmid cAMP-response element binding protein-luciferase (pCRE-luc) reporter along with plasmid Cytomegalovirus (pCMV)-Renilla. Eighteen hours after transfection, cells were treated with compound or BAs extracted from serum. Cells were harvested 6 hours later for the luciferase assays using the Luciferase Assay System (Promega). Luciferase activity was normalized to renilla activity.

Western Blot

Protein was extracted from cells or tissues using the M-PER Mammalian Protein Extraction Reagent (78501; Thermo Fisher, Waltham, MA) or the T-PER Tissue Protein Extraction Reagent (78510; Thermo Fisher) containing protease/phosphatase inhibitor cocktail (P8340, P0044; Sigma). Antibodies against UCP1 (10983, 1:1000; Abcam), adipose triglyceride lipase (3A04, 2439S, 1:1000; Cell Signaling Technology), heat shock protein 90 (C45G5, 4877S, 1:1000; Cell Signaling Technology), and TGR5 (72608, 1:1000; Abcam) were used.

Quantitative Real-Time Polymerase Chain Reaction

Total RNA was extracted from tissues and cells using TRIzol reagent (TR118; MRC, Cincinnati, OH). The RNA was reverse-transcribed using Complementary DNA Synthesis SuperMix (Invitrogen, Waltham, MA). Quantitative real-time polymerase chain reaction (PCR) was performed with SYBR Green PCR Master Mix (Applied Biosystems, Waltham, MA) using an ABI 7900HT Fast Real-Time PCR System (Applied Biosystems). The sequences of primers used are listed in [Table 2](#). mRNA levels were normalized to 36B4.

Indirect Calorimetry and Locomotor Activity Assays

Mice were placed in comprehensive animal metabolic monitoring system cages (Columbus Instruments, Columbus, OH). The volume of O₂ consumption and CO₂ production were recorded over a 48-hour period. Energy expenditure was calculated as described.⁴⁵

Fatty Acid Oxidation Assay

Fatty acid oxidation of BAT was measured using a fatty acid oxidation Assay Kit (E-141; BRSC, Buffalo, NY).

BAT-Specific TGR5 Knockdown

The AAV plasmid was constructed by the ligation of a synthetic mini-UCP1 promoter and enhancer sequence from Twist Bioscience (San Francisco, CA) as previously reported,^{47–49} the *CasRx* gene from pXR001 (109049; Addgene, Watertown, MA), bovine growth hormone polyadenylation(bGH polyA) sequence, and a human U6 promoter driven DR30-sgRNA cassette into an AAV backbone. The sequence of TGR5 sgRNA is AAACGTAGTAGGCTTAG-GAAGAAGCAGAAAAGTCTTCTTCCTAAGCCTACTAC. The plasmids for the AAV2/9 system were used for the BAT-specific KD of TGR5 in vivo.^{50,51} This system contains a transgene plasmid with a UCP1 enhancer and promoter and TGR5 sgRNA placed between the two 145-base inverted terminal repeats (ITRs) (from type 2 AAV), a transfer plasmid with sequences coding for replication gene (REP, from type 2 AAV) and capsid gene (CAP, from type 9 AAV), and a helper plasmid with E4, E2a, and virus-associated (VA, from adenovirus). The plasmids were mixed and transfected into HEK 293T cells. The cells and the medium containing packaged viruses were collected 72 hours after transfection. The cells then were lysed through 3 rounds of freezing in ethanol/dry ice, followed by thawing in a 37°C water bath. Next, 5× polyethylene glycol (40% polyethylene glycol-8000, 2.5 mol/L NaCl) was added to the medium to a final concentration of 8% polyethylene glycol-8000 and 0.5 mol/L NaCl, stirred for 1 hour, and then incubated overnight at 4°C. After centrifugation, the cell lysates and the polyethylene glycol pellet were mixed. The mixture was purified in 15%, 25%, 40%, and 60% iodixanol (Sigma-Aldrich) gradients by ultracentrifugation. The viruses were extracted from the 40% iodixanol gradient and washed 3 times with phosphate-buffered saline in ultrafiltration tubes through centrifugation. The copy numbers of AAV were determined by quantitative PCR (Applied Biosystems); AAV (1 × 10¹² copies per mouse) were injected into 4-week-old C57BL/6J (WT) female mice via tail vein. Three to 4 weeks later, mice were subjected to alcohol-induced AALD in the same method as performed for TGR5 KO mice.

Statistical Analysis

Statistical analyses were performed using GraphPad Prism (version 8). All data are expressed as means ± SEM. Statistical significance was analyzed using an unpaired Student *t* test or 1-way analysis of variance with the Dunn post-test. The threshold of statistical significance was set at *P* < .05.

All authors had access to the study data and reviewed and approved the final manuscript.

References

- Crabb DW, Im GY, Szabo G, Mellinger JL, Lucey MR. Diagnosis and treatment of alcohol-related liver

- diseases: 2019 Practice Guidance from the American Association for the Study of Liver Diseases. *Hepatology* 2020;71:306–333.
- You M, Arteel GE. Effect of ethanol on lipid metabolism. *J Hepatol* 2019;70:237–248.
 - Seitz HK, Bataller R, Cortez-Pinto H, Gao B, Gual A, Lackner C, Mathurin P, Mueller S, Szabo G, Tsukamoto H. Alcoholic liver disease. *Nat Rev Dis Primers* 2018;4:16.
 - Yuan J, Chen C, Cui J, Lu J, Yan C, Wei X, Zhao X, Li N, Li S, Xue G, Cheng W, Li B, Li H, Lin W, Tian C, Zhao J, Han J, An D, Zhang Q, Wei H, Zheng M, Ma X, Li W, Chen X, Zhang Z, Zeng H, Ying S, Wu J, Yang R, Liu D. Fatty liver disease caused by high-alcohol-producing *Klebsiella pneumoniae*. *Cell Metab* 2019;30:675–688 e7.
 - Buzzetti E, Kalafateli M, Thorburn D, Davidson BR, Thiele M, Gluud LL, Del Giovane C, Askgaard G, Krag A, Tsochatzis E, Gurusamy KS. Pharmacological interventions for alcoholic liver disease (alcohol-related liver disease): an attempted network meta-analysis. *Cochrane Database Syst Rev* 2017;3:CD011646.
 - Haussinger D, Keitel V. Dual role of the bile acid receptor Takeda G-protein-coupled receptor 5 for hepatic lipid metabolism in feast and famine. *Hepatology* 2017;65:767–770.
 - Brandl K, Hartmann P, Jih LJ, Pizzo DP, Argemi J, Ventura-Cots M, Coulter S, Liddle C, Ling L, Rossi SJ, DePaoli AM, Loomba R, Mehal WZ, Fouts DE, Lucey MR, Bosques-Padilla F, Mathurin P, Louvet A, Garcia-Tsao G, Verna EC, Abralde JG, Brown RS Jr, Vargas V, Altamirano J, Caballeria J, Shawcross D, Starkel P, Ho SB, Bataller R, Schnabl B. Dysregulation of serum bile acids and FGF19 in alcoholic hepatitis. *J Hepatol* 2018;69:396–405.
 - Xie G, Zhong W, Li H, Li Q, Qiu Y, Zheng X, Chen H, Zhao X, Zhang S, Zhou Z, Zeisel SH, Jia W. Alteration of bile acid metabolism in the rat induced by chronic ethanol consumption. *FASEB J* 2013;27:3583–3593.
 - Manley S, Ding W. Role of farnesoid X receptor and bile acids in alcoholic liver disease. *Acta Pharm Sin B* 2015;5:158–167.
 - Gong X, Zhang Q, Ruan Y, Hu M, Liu Z, Gong L. Chronic alcohol consumption increased bile acid levels in enterohepatic circulation and reduced efficacy of irinotecan. *Alcohol Alcohol* 2020;55:264–277.
 - Donepudi AC, Ferrell JM, Boehme S, Choi HS, Chiang JYL. Deficiency of cholesterol 7 α -hydroxylase in bile acid synthesis exacerbates alcohol-induced liver injury in mice. *Hepatol Commun* 2018;2:99–112.
 - Kong B, Zhang M, Huang M, Rizzolo D, Armstrong LE, Schumacher JD, Chow MD, Lee YH, Guo GL. FXR deficiency alters bile acid pool composition and exacerbates chronic alcohol induced liver injury. *Dig Liver Dis* 2019;51:570–576.
 - Reich M, Klindt C, Deutschmann K, Spomer L, Haussinger D, Keitel V. Role of the G protein-coupled bile acid receptor TGR5 in liver damage. *Dig Dis* 2017;35:235–240.
 - Merlen G, Kahale N, Ursic-Bedoya J, Bidault-Jourdainne V, Simerabet H, Doignon I, Tanfin Z, Garcin I, Pean N, Gautherot J, Davit-Spraul A, Guettier C, Humbert L, Rainteau D, Ebnet K, Ullmer C, Cassio D, Tordjmann T. TGR5-dependent hepatoprotection through the regulation of biliary epithelium barrier function. *Gut* 2020;69:146–157.
 - Wang YD, Chen WD, Yu D, Forman BM, Huang W. The G-protein-coupled bile acid receptor, Gpbar1 (TGR5), negatively regulates hepatic inflammatory response through antagonizing nuclear factor kappa light-chain enhancer of activated B cells (NF- κ B) in mice. *Hepatology* 2011;54:1421–1432.
 - Potthoff MJ, Potts A, He T, Duarte JA, Taussig R, Mangelsdorf DJ, Kliewer SA, Burgess SC. Colesevelam suppresses hepatic glycogenolysis by TGR5-mediated induction of GLP-1 action in DIO mice. *Am J Physiol Gastrointest Liver Physiol* 2013;304:G371–G380.
 - Lou GY, Ma XX, Fu XH, Meng ZP, Zhang WY, Wang YD, Van Ness C, Yu DN, Xu RZ, Huang WD. GPBAR1/TGR5 mediates bile acid-induced cytokine expression in murine Kupffer cells. *PLoS One* 2014;9:e93567.
 - Shen H, Jiang L, Lin JD, Omary MB, Rui L. Brown fat activation mitigates alcohol-induced liver steatosis and injury in mice. *J Clin Invest* 2019;129:2305–2317.
 - Broeders EP, Nascimento EB, Havekes B, Brans B, Roumans KH, Tailleux A, Schaart G, Kouach M, Charton J, Deprez B, Bouvy ND, Mottaghy F, Staels B, van Marken Lichtenbelt WD, Schrauwen P. The bile acid chenodeoxycholic acid increases human brown adipose tissue activity. *Cell Metab* 2015;22:418–426.
 - Watanabe M, Houten SM, Matakai C, Christoffolete MA, Kim BW, Sato H, Messaddeq N, Harney JW, Ezaki O, Kodama T, Schoonjans K, Bianco AC, Auwerx J. Bile acids induce energy expenditure by promoting intracellular thyroid hormone activation. *Nature* 2006;439:484–489.
 - Jacinto S, Fang S. Essential roles of bile acid receptors FXR and TGR5 as metabolic regulators. *Anim Cells Syst* 2014;18:359–364.
 - Jin LH, Fang ZP, Fan MJ, Huang WD. Bile-ology: from bench to bedside. *J Zhejiang Univ Sci B* 2019;20:414–427.
 - Spatz M, Ciocan D, Merlen G, Rainteau D, Humbert L, Gomes-Rochette N, Hugot C, Trainel N, Mercier-Nomé F, Domenichini S, Puchois V, Wrzosek L, Ferrere G, Tordjmann T, Perlemuter G, Cassard A-M. Bile acid-receptor TGR5 deficiency worsens liver injury in alcohol-fed mice by inducing intestinal microbiota dysbiosis. *JHEP Rep* 2021;3:100230.
 - Miyata T, Nagy LE. Programmed cell death in alcohol-associated liver disease. *Clin Mol Hepatol* 2020;26:618–625.
 - Bertola A, Mathews S, Ki SH, Wang H, Gao B. Mouse model of chronic and binge ethanol feeding (the NIAAA model). *Nat Protoc* 2013;8:627–637.
 - Strable MS, Ntambi JM. Genetic control of de novo lipogenesis: role in diet-induced obesity. *Crit Rev Biochem Mol Biol* 2010;45:199–214.

27. Zhong W, Zhao Y, Tang Y, Wei X, Shi X, Sun W, Sun X, Yin X, Sun X, Kim S, McClain CJ, Zhang X, Zhou Z. Chronic alcohol exposure stimulates adipose tissue lipolysis in mice: role of reverse triglyceride transport in the pathogenesis of alcoholic steatosis. *Am J Pathol* 2012;180:998–1007.
28. Zhao C, Liu Y, Xiao J, Liu L, Chen S, Mohammadi M, McClain CJ, Li X, Feng W. FGF21 mediates alcohol-induced adipose tissue lipolysis by activation of systemic release of catecholamine in mice. *J Lipid Res* 2015;56:1481–1491.
29. Donepudi AC, Boehme S, Li F, Chiang JYL. G-protein-coupled bile acid receptor plays a key role in bile acid metabolism and fasting-induced hepatic steatosis in mice. *Hepatology* 2017;65:813–827.
30. Feldmann HM, Golozoubova V, Cannon B, Nedergaard J. UCP1 ablation induces obesity and abolishes diet-induced thermogenesis in mice exempt from thermal stress by living at thermoneutrality. *Cell Metab* 2009;9:203–209.
31. Yu DD, Sousa KM, Mattern DL, Wagner J, Fu X, Vaidehi N, Forman BM, Huang W. Stereoselective synthesis, biological evaluation, and modeling of novel bile acid-derived G-protein coupled bile acid receptor 1 (GPBAR1, TGR5) agonists. *Bioorg Med Chem* 2015;23:1613–1628.
32. Maruyama T, Tanaka K, Suzuki J, Miyoshi H, Harada N, Nakamura T, Miyamoto Y, Kanatani A, Tamai Y. Targeted disruption of G protein-coupled bile acid receptor 1 (Gpbar1/M-Bar) in mice. *J Endocrinol* 2006;191:197–205.
33. Sugita T, Amano K, Nakano M, Masubuchi N, Sugihara M, Matsuura T. Analysis of the serum bile acid composition for differential diagnosis in patients with liver disease. *Gastroenterol Res Pract* 2015;2015:717431.
34. Parker R, Kim SJ, Gao B. Alcohol, adipose tissue and liver disease: mechanistic links and clinical considerations. *Nat Rev Gastroenterol Hepatol* 2018;15:50–59.
35. Hwang S, Gao B. How does your fat affect your liver when you drink? *J Clin Invest* 2019;129:2181–2183.
36. Sebastian BM, Roychowdhury S, Tang H, Hillian AD, Feldstein AE, Stahl GL, Takahashi K, Nagy LE. Identification of a cytochrome P450E1/Bid/C1q-dependent axis mediating inflammation in adipose tissue after chronic ethanol feeding to mice. *J Biol Chem* 2011;286:35989–35997.
37. Huttunen P, Kortelainen ML. Long-term alcohol consumption and brown adipose tissue in man. *Eur J Appl Physiol Occup Physiol* 1990;60:418–424.
38. Huttunen P, Kortelainen ML. Chronic alcohol intake induces the oxidative capacity of brown adipose tissue in the rat. *Pharmacol Biochem Behav* 1988;29:53–57.
39. Yoshimoto K, Yasuhara M, Komura S, Misumi Y, Uchiyama Y, Kogure A, Hioki C, Wakabayashi Y, Satomi Y, Nishimura A, Fukuda F, Hori M, Yokoyama C, Yoshida T. Effects of ethanol on the induction of uncoupling protein-1 (UCP1) mRNA in the mouse brown adipose tissue. *Tohoku J Exp Med* 2004;204:45–51.
40. Gioiello A, Rosatelli E, Nuti R, Macchiarulo A, Pellicciari R. Patented TGR5 modulators: a review (2006 - present). *Expert Opin Ther Pat* 2012;22:1399–1414.
41. Iracheta-Vellve A, Calenda CD, Petrasek J, Ambade A, Kodys K, Adorini L, Szabo G. FXR and TGR5 agonists ameliorate liver injury, steatosis, and inflammation after binge or prolonged alcohol feeding in mice. *Hepatology* 2018;2:1379–1391.
42. Hartmann P, Seebauer CT, Schnabl B. Alcoholic liver disease: the gut microbiome and liver crosstalk. *Alcohol Clin Exp Res* 2016;39:763–775.
43. Vassileva G, Golovko A, Markowitz L, Abbondanzo SJ, Zeng M, Yang S, Hoos L, Tetzloff G, Levitan D, Murgolo NJ, Keane K, Davis HR Jr, Hedrick J, Gustafson EL. Targeted deletion of Gpbar1 protects mice from cholesterol gallstone formation. *Biochem J* 2006;398:423–430.
44. Khanova E, Wu R, Wang W, Yan R, Chen Y, French SW, Lorente C, Pan SQ, Yang Q, Li Y, Lazaro R, Ansong C, Smith RD, Bataller R, Morgan T, Schnabl B, Tsukamoto H. Pyroptosis by caspase 11/4-gasdermin-D pathway in alcoholic hepatitis in mice and patients. *Hepatology* 2018;67:1737–1753.
45. Ding L, Sousa KM, Jin L, Dong B, Kim BW, Ramirez R, Xiao Z, Gu Y, Yang Q, Wang J, Yu D, Pigazzi A, Schones D, Yang L, Moore D, Wang Z, Huang W. Vertical sleeve gastrectomy activates GPBAR-1/TGR5 to sustain weight loss, improve fatty liver, and remit insulin resistance in mice. *Hepatology* 2016;64:760–773.
46. Lu Y, Zheng WL, Lin SC, Guo FS, Zhu YL, Wei YJ, Liu X, Jin SK, Jin LH, Li Y. Identification of an oleanane-type triterpene hedragonic acid as a novel farnesoid X receptor ligand with liver protective effects and anti-inflammatory activity. *Mol Pharmacol* 2018;93:63–72.
47. Larose M, Cassard-Doulcier AM, Fleury C, Serra F, Champigny O, Bouillaud F, Ricquier D. Essential cis-acting elements in rat uncoupling protein gene are in an enhancer containing a complex retinoic acid response domain. *J Biol Chem* 1996;271:31533–31542.
48. Cassard-Doulcier AM, Gelly C, Bouillaud F, Ricquier D. A 211-bp enhancer of the rat uncoupling protein-1 (UCP-1) gene controls specific and regulated expression in brown adipose tissue. *Biochem J* 1998;333:243–246.
49. Cassard-Doulcier AM, Gelly C, Fox N, Schrementi J, Raimbault S, Klaus S, Forest C, Bouillaud F, Ricquier D. Tissue-specific and beta-adrenergic regulation of the mitochondrial uncoupling protein gene: control by cis-acting elements in the 5'-flanking region. *Mol Endocrinol* 1993;7:497–506.
50. Jimenez V. In vivo adeno-associated viral vector-mediated genetic engineering of white and brown adipose tissue in adult mice. *Diabetes* 2013;62:4012–4022.
51. Shi M, Huang XY, Ren XY, Wei XY, Ma Y, Lin ZZ, Liu DT, Song L, Zhao TJ, Li G, Yao L, Zhu M, Zhang C, Xie C, Wu Y, Wu HM, Fan LP, Ou J, Zhan YH, Lin SY, Lin SC.

AIDA directly connects sympathetic innervation to adaptive thermogenesis by UCP1. *Nat Cell Biol* 2021; 23:268–277.

Received April 29, 2021. Accepted December 1, 2021.

Correspondence

Address correspondence to: Wendong Huang, PhD, Department of Diabetes Complications and Metabolism, Beckman Research Institute, City of Hope National Medical Center, Duarte, California 91010. e-mail: WHuang@coh.org; fax: (626) 256-8704. Qingfeng Yan, PhD, College of Life Science, Zhejiang University, Hangzhou, 310058 Zhejiang, China. e-mail: qfyan@zju.edu.cn; fax: 01186-571-88206646.

CRedit Authorship Contributions

Mingjie Fan, PhD (Data curation: Lead; Formal analysis: Lead; Investigation: Lead; Methodology: Lead; Writing – original draft: Lead)

Yangmeng Wang (Data curation: Supporting; Investigation: Supporting; Methodology: Supporting; Project administration: Supporting)

Lihua Jin, PhD (Conceptualization: Supporting; Formal analysis: Supporting; Supervision: Supporting; Visualization: Supporting; Writing – review & editing: Lead)

Zhipeng Fang (Investigation: Supporting; Project administration: Supporting)

Jiangling Peng, PhD (Data curation: Supporting; Methodology: Supporting)
Jui Tu (Investigation: Supporting; Project administration: Supporting)

YanJun Liu, PhD (Data curation: Supporting; Project administration: Supporting)

Eryun Zhang, PhD (Investigation: Supporting; Project administration: Supporting)

Senlin Xu, PhD (Data curation: Supporting; Methodology: Supporting)

Xiaoqian Liu, PhD (Methodology: Supporting)

Yuqing Huo (Data curation: Supporting)

Zhaoli Sun (Funding acquisition: Supporting; Methodology: Supporting)

Xiaojuan Chao (Methodology: Supporting)

Wenxing Ding, PhD (Funding acquisition: Supporting; Methodology: Supporting)

Qingfeng Yan, PhD (Conceptualization: Lead; Funding acquisition: Equal; Project administration: Equal; Supervision: Equal; Writing – review & editing: Supporting)

Wendong Huang, PhD (Conceptualization: Lead; Funding acquisition: Lead; Project administration: Lead; Supervision: Lead; Writing – original draft: Lead; Writing – review & editing: Lead)

Conflicts of interest

The authors disclose no conflicts.

Funding

This study was supported by the Schaeffer Foundation, the Hench Foundation, National Institutes of Health grants R01DK124627 and COH P30CA33572 (W.H.), R24 AA025017 (Z.S.), and R37AA020518, U01AA024733, and R01AG072895 (W.-X.D.); and the National Natural Science Foundation of China grants 31771398 and 32070584 (Q.Y.).